2010

Piezoelectric tuning of exchange bias in a $BaTiO_3/Co/CoO$ heterostructure

Srinivas Polisetty
University of Nebraska-Lincoln, polisetty.srinivas@gmail.com

W. Echtenkamp
University of Nebraska-Lincoln

Keith Jones
University of Nebraska-Lincoln, keith.jones@huskers.unl.edu

X. He
University of Nebraska-Lincoln

Sarbeswar Sahoo
University of Nebraska-Lincoln, sarbeswar@gmail.com

See next page for additional authors

Piezoelectric tuning of exchange bias in a $BaTiO_3$/Co/CoO heterostructure

S. Polisetty,[1] W. Echtenkamp,[1] K. Jones,[1] X. He,[1] S. Sahoo,[2] and Ch. Binek[1,*]
[1]*Department of Physics and Astronomy and the Nebraska Center for Materials and Nanoscience, University of Nebraska, Lincoln, Nebraska 68588-0111, USA*
[2]*Seagate Technology, Minneapolis, Minnesota 55435, USA*
(Received 16 April 2010; revised manuscript received 22 June 2010; published 12 October 2010)

Piezoelectrically controlled strain is used for electric tuning of exchange-bias fields. A generic exchange-bias Co/CoO bilayer is deposited on the surface of a ferroelectric and thus piezoelectric $BaTiO_3$ substrate which allows to apply electrically and thermally tunable stress in the adjacent ferromagnetic Co thin film. The stress-induced strain alters foremost the magnetic anisotropy of the Co film and by that the magnetization orientation at the Co/CoO interface modifying the exchange-bias field. This results in a pronounced electrically induced weakening of the exchange bias but also includes the possibility of tuning the exchange-bias field through a subtle sign change from regular negative to positive values. The electrically controlled crossover from negative to positive exchange bias is consistently observed at various temperatures in the rhombohedral phase of $BaTiO_3$. This complex electric field dependence of the exchange-bias field is the result of the long-range nature of strain and interpreted through competition between ferromagnetic and antiferromagnetic exchange at the Co/CoO interface. Our data suggest competition between regular negative and positive exchange bias. Weakening of negative exchange bias originates from noncollinear alignment of the Co and CoO interface magnetizations. Positive exchange bias is activated when stress induces antiferromagnetic exchange through atomic displacements changing the exchange paths at the Co/CoO interface.

DOI: 10.1103/PhysRevB.82.134419 PACS number(s): 75.70.Cn, 75.80.+q, 77.84.−s

I. INTRODUCTION

At the hub of high-performance information technology is the realization of advanced nonvolatile memory devices.[1–3] At present, one of the competitively performing technologies is the magnetic random access memory (MRAM) (Ref. 4) that utilizes the switchable relative orientation of the magnetization in a ferromagnetic (FM) layer. The switchable sensor layer is separated by a nonmagnetic spacer from a second, pinned FM layer. The latter in turn is in atomic proximity of an antiferromagnetic (AF) layer which gives rise to pinning of the FM magnetization in magnitude and orientation. This magnetic coupling phenomenon is known as exchange bias (EB).[5–11] It is an interface phenomenon of basic scientific interest and crucial for spintronic devices such as the MRAM. Electric control of EB promises numerous potential spintronic applications beyond passive MRAM technology.[12]

EB in FM/AF heterostructures requires an initialization process by magnetic field cooling of the bilayer to below the blocking temperature, T_B, of the AF thin film. The most remarkable and widely studied feature of EB systems is the pinning effect exploited in magnetic field sensors and MRAMs. It manifests itself through a shift of the FM hysteresis loop of the pinned ferromagnet along the magnetic field axis by the EB field, $\mu_0 H_{EB}$. EB effects in FM/AF bilayers have been widely studied.[13–15] Numerous investigations on various systems reveal details of the dependences of EB on temperature,[16] thicknesses of both antiferromagnet[17] and ferromagnet,[16] anisotropy,[18] and roughness at the interface,[19] to name just a few. In addition, an aging phenomenon has been observed and extensively studied in various EB systems.[16,20–25] This nonequilibrium phenomenon manifests itself by a gradual but incomplete degradation of the EB field upon cycling of the pinned ferromagnet through consecutive hysteresis loops, n. The phenomenon is known as training effect and is quantified by $\mu_0 H_{EB}$ vs n. The training effect can be considered in a more general framework and its theoretical description has been successfully transferred from FM/AF systems to FM bilayer structures where a magnetically soft ferromagnet is antiferromagnetically coupled with a hard ferromagnet through Ruderman-Kittel-Kasuya-Yoshida coupling tuned via the thickness of a nonmagnetic spacer.[26–31] While much work has been dedicated to achieving a fundamental understanding of EB,[5,32,33] rather little effort has been invested into finding novel and improved ways of controlling EB. Extrinsic control of EB is of importance for spintronic device applications. In this paper we describe a route toward controlling exchange bias electrically using piezoelectrically tuned stress as the control parameter.

The physics of electric field control of EB has been pioneered in perpendicular EB systems using the magnetoelectric antiferromagnet, Cr_2O_3 as active pinning system.[12,34–36] Later single-phase multiferroic pinning layers such as $BiFeO_3$ have been used taking advantage of the direct electric control of the ferroelectric polarization which shows coupling to the AF order parameter.[37–43] Despite clear experimental identification of electrically controlled EB, the overall level of controllability has still limitations asking for alternative approaches.

In addition to the technological relevance, electric control of EB can help to deepen the basic understanding of the EB phenomenon in general and the controlled EB based on magnetoelectric and multiferroic pinning systems in particular. In this paper, we present a third path of electrically controlled EB where we exploit the piezoelectric property of a ferroelectric material to tune the EB and coercivity in FM/AF bilayers and study the interface magnetism of the EB heterostructure from a new perspective. We distinguish two different mechanisms which, when acting in concert, enable elec-

tric control of EB: (i) the piezoelectricity of the ferroelectric $BaTiO_3$ (BTO) substrate allows for electrically controlled stress primarily in the adjacent FM Co layer[44–48] changing the magnetic anisotropy of the Co layer via the magnetoelastic anisotropy contribution, (ii) EB at the FM/AF interface[5–11,49,50] which depends on the relative orientation of the FM and AF interface magnetizations and the effective exchange at the interface both of which are controllably affected by the piezoelectrically induced strain.

There have been plenty of studies on piezoelectrically controlled magnetoelastic anisotropy changes[51–54] as well as the dependence of EB on interface exchange and magnetization; however, to the best of our knowledge, these two effects have never been exploited together. Therefore, here we study the piezoelectric control of EB, EB training, and FM coercivity in a piezoelectric/ferromagnetic/antiferromagnetic heterostructure.

II. SAMPLE PREPARATION AND STRUCTURAL CHARACTERIZATION

We use molecular-beam epitaxy to grow a hexagonal Co thin film with (0001) texture on top of a single-crystalline substrate of tetragonal $BaTiO_3$. The growth process starts from a base pressure of 5.0×10^{-11} mbar prior to deposition. The BTO substrate is heated under ultrahigh-vacuum conditions and kept at 573 K for 10 min to clean the BTO surface from physisorbed molecular contaminations. Later the temperature is decreased and maintained at 373 K for the Co deposition via thermal evaporation. At this substrate temperature, the tetragonal structure of the BTO is stabilized as a reference phase for the Co deposition. A thin film of 5.0 nm of Co is deposited at a growth rate of 0.48 nm/min. The chamber pressure during growth reached 3.0×10^{-9} mbar. After the Co deposition, the sample is exposed to *ex situ* atmospheric conditions where a CoO thin film of about 3.0 nm is formed on top of the Co thin film.

BTO is a prototypical ferroelectric material[55,56] which has been used previously by some of us to study the piezoelectric control of the anisotropy and coercivity in a BTO/Fe heterostructure.[44] We build on this experience for the more complex investigation of the piezoelectrically controlled EB reported here. The well investigated Co/CoO bilayer system is utilized for the purpose of generating EB.[57–62] Structural characterization of our BTO/Co/CoO heterostructure has been performed by θ-2θ wide-angle x-ray diffraction (XRD) using the Cu $K\alpha$ source of our Rigaku D/Max-B diffractometer. The XRD pattern of Fig. 1 reveals a single-crystalline hexagonal Co film with (0001)-oriented growth on top of the tetragonal BTO substrate with (001) cut. The wide-angle XRD shows no signature of the CoO film. However, small-angle x-ray reflectivity (XRR) performed by a Bruker-AXS D8 machine is able to identify a layer of 3.0 nm CoO which is naturally formed on top of the Co thin film. Likewise, the thickness of the Co layer is determined from the same XRR scan. A thickness of 5.0 nm is evaluated via best-fit analysis using the LEPTOS-2 software.

III. MAGNETIC CHARACTERIZATION

The magnetic response of the BTO/Co/CoO heterostructure with varying temperatures (Figs. 2 and 3) and electric

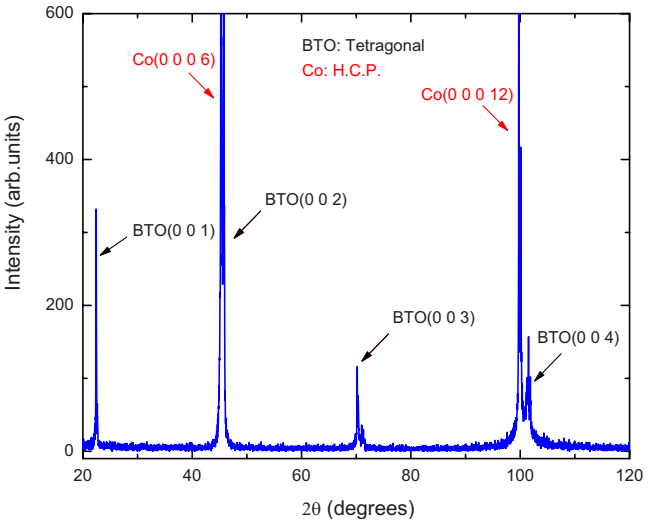

FIG. 1. (Color online) X-ray diffraction pattern of the Co/CoO bilayer on $BaTiO_3$ substrate. Single-crystalline peaks of hexagonal Co film and tetragonal $BaTiO_3$ are identified.

fields (Figs. 4 and 5) are measured by a superconducting quantum interference device (SQUID) magnetometer (Quantum Design, MPMS-XL) and longitudinal magneto-optical Kerr effect (L-MOKE), respectively.[63] The temperature dependence of in-plane [Fig. 2(a)] and out-of-plane [Fig. 2(b)] magnetizations, $M_{\parallel}$ vs T and $M_{\perp}$ vs T, were measured in small magnetic fields of $\mu_0 H=1$ mT (circles) and 10 mT (squares) after field cooling the sample from $T=400$ K to $T=10$ K in a saturation field of $\mu_0 H=200$ mT applied in the

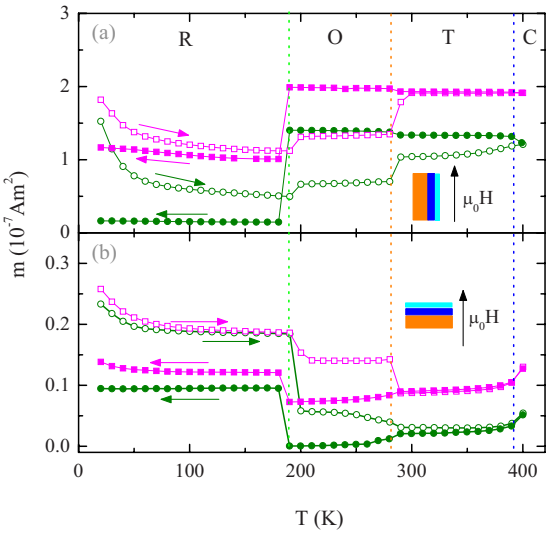

FIG. 2. (Color online) (a) Variation in the Co film (a) in-plane magnetization, $M_{\parallel}$ (b) out-of-plane magnetization, $M_{\perp}$ with temperature, T, at magnetic fields, $\mu_0 H=1$ mT (circles) and 10 mT (squares). Open and solid symbols are $\mu_0 H$-heating and $\mu_0 H$-cooling curves, respectively. Arrows point to the direction of temperature scans across rhombohedral (R), orthorhombic (O), tetragonal (T), and cubic (C) phases of $BaTiO_3$. Dotted lines are the boundaries between respective phase transitions. The insets depict the layered sample structure with arrows pointing in the direction of applied magnetic field, respectively.

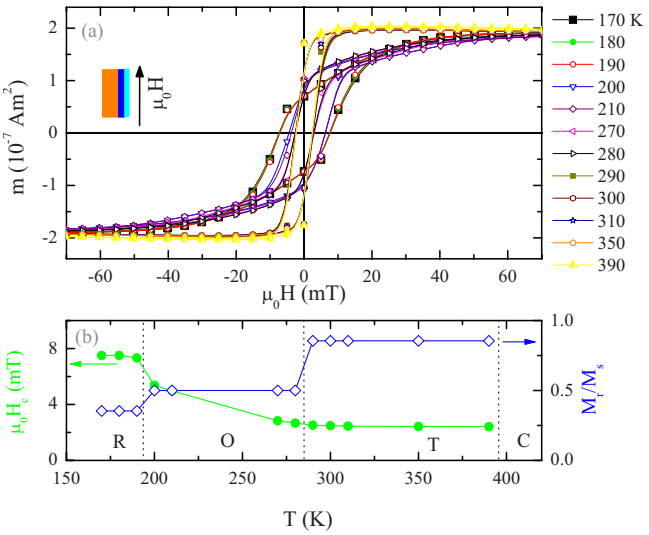

FIG. 3. (Color online) (a) In-plane magnetic hysteresis loops, M vs $\mu_0 H$, at various temperatures $170 < T < 390$ K measured upon heating after initial zero-field cooling to 170 K. (b) Coercivity, $\mu_0 H_c$ (spheres) and ratio of remanent to saturation magnetization, M_r/M_s (triangles) vs T *as* obtained from the loops in (a).

plane and out of the plane of the sample, respectively. All temperature-dependent magnetization measurements have been done in zero electric field. Similar to our earlier reported results[44] on BTO/Fe, M vs T shows three abrupt magnetization discontinuities at temperatures $T \approx 393$, 278, and 190 K which are associated with BTO structural phase transitions of cubic-tetragonal (C→T), tetragonal-orthorhombic (T→O), and orthorhombic-rhombohedral (O→R), respectively. The structural transitions give rise to changes in the

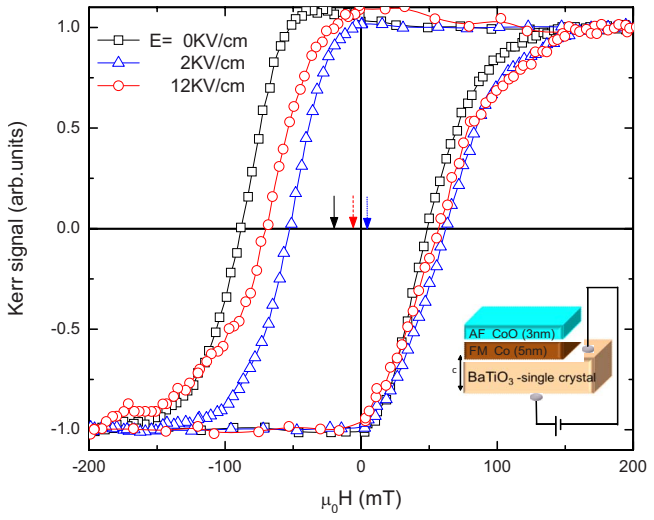

FIG. 4. (Color online) Normalized Kerr magnetic loops, $-0.25 \leq \mu_0 H \leq 0.25$ T, measured after the sample is cooled from $T=320$ K to $T=40$ K in the presence of a magnetic field $\mu_0 H=0.25$ T and electric fields, $E=0$ kV/cm (black squares), 2 kV/cm (blue triangles), and 12 kV/cm (red circles), respectively. Solid, dotted, and dashed arrows indicate the values of $\mu_0 H_{EB}$ for the respective E fields. The inset depicts a cartoon of the sample with reference axis and E-field contacting.

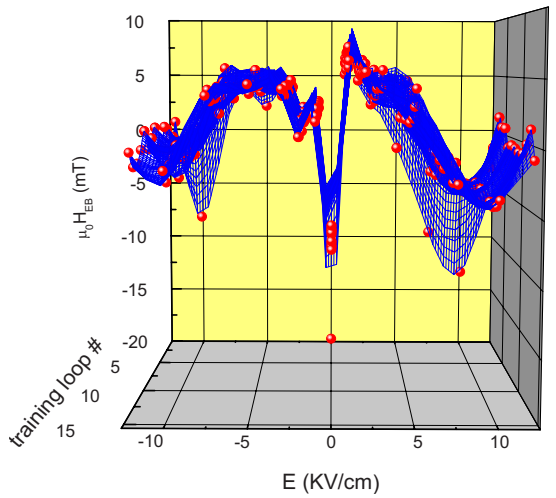

FIG. 5. (Color online) 3D plot of the exchange bias $\mu_0 H_{EB}$ vs applied electric field E and training loop number n. The spheres are the experimental data obtained from Fig. 4 and other E fields (not shown). The interpolating eye-guiding grid results from Renka-Cline gridding algorithm.

stress experienced by the adjacent Co layer. Therefore, the magnetic anisotropy of the top Co film is strongly modified via magnetoelastic coupling at the interface. This gives rise to reorientation of the Co magnetization from in-plane (out-of-plane) to preferentially out-of-plane (in-plane) orientation when field cooling (field heating), respectively.[64–67] As noticed from Figs. 2(a) and 2(b) the magnetization discontinuities at $\mu_0 H=10$ mT are less pronounced than those at $\mu_0 H=1$ mT. This reflects the increasing importance of the Zeeman energy, $E_{Zeeman}=-MV\,\mu_0 H$, of the FM Co volume V in larger magnetic fields in comparison with the anisotropy energy and, in particular, its magnetoelastic contribution, $E_{me}=K_{me}\sin^2\theta$. Here θ measures the angle between the magnetization and the in-plane stress indicating out-of-plane preferential orientation for a magnetoelastic anisotropy constant $K_{me}<0$.

In-plane magnetic hysteresis loops, M vs $\mu_0 H$, are measured at various temperatures, $170 < T < 390$ K in zero electric field. All hysteresis loops are measured upon heating the sample after initially zero-field cooling to 170 K. The hysteresis loops reveal profound changes in the coercivity, $\mu_0 H_c$, and ratio of remanent to saturation magnetization, M_r/M_s, of the Co/CoO heterostructure as plotted in Figs. 3(a) and 3(b), respectively. This signifies the modification of the magnetic properties of Co due to the magnetoelastic coupling at the interface between BTO and Co. Here the strain is thermally controlled via the temperature-dependent structural transitions of BTO. The coercivity in Fig. 3(b) shows discontinuities at the structural phase transition of BTO, in particular, at the phase transition of R→O similar to our earlier reports of Ref. 44. Note however, that M_r/M_s shows a sudden increase at R→O phase transition of BTO unlike to the magnetization in the BTO/Fe sample discussed in Ref. 44 indicating an opposite sign in the effective magnetoelastic constant K_{me}. Moreover, it can be seen that M_r of Co is almost constant within one phase of BTO and only changes at the structural phase transition of BTO. Also the remanent magnetization in

Fig. 3(b) has the propensity to follow the magnetization of the magnetic field-heating branch (open symbols) in Fig. 2(a).

Temperature-controlled strain effects provide interesting insights in the strain dependence of the anisotropy, coercivity, and EB of our heterosystem. However, it is technologically more appealing to perceive voltage controlled magnetism, in particular, electrically controlled EB, motivated by potential spintronic applications.[12] We use L-MOKE (Ref. 63) for the magnetic studies with electrical fields applied along the c axis in the tetragonal phase of the 1-mm-thick BTO substrate. Gold wires are contacted with the help of silver paste covering the entire bottom surface of BTO (5×5 mm^2) and less than half of the top surface of BTO ($\sim2\times5$ mm^2) as shown in the inset of Fig. 4. We apply silver paste only on a portion of the top surface such that the remaining surface can be used for the Kerr measurements without perturbation through the silver past. Specifically, a laser beam of 670 nm wavelength is focused on the entire uncovered portion of the Co/CoO film and 15 consecutive in-plane magnetic hysteresis loops with magnetic fields $-0.25\leq\mu_0H\leq0.25$ T are measured as described elsewhere.[16]

IV. EXPERIMENTAL RESULTS AND DISCUSSION

EB field values are determined from L-MOKE hysteresis loops after cooling the heterostructure from $T=320$ K in the presence of $E=0$ (squares), 2 (triangles), and 12 kV/cm (circles), and the simultaneously applied magnetic field, $\mu_0H=0.25$ T. Typical results are displayed in Fig. 4 for isothermal hysteresis loops at $T=40$ K. The particular loop corresponding to $E=0$ kV/cm (squares) shows a regular negative EB loop shift of $\mu_0H_{\mathrm{EB}}=-19.5$ mT indicated by a black arrow in Fig. 4. Its value is consistent with our earlier reported results of Co/CoO EB heterosystems deposited on sapphire.[16] The Co hysteresis loop shifts along the μ_0H axis to a positive value of $\mu_0H_{\mathrm{EB}}=4.5$ mT with the application of the positive electric field, $E=2$ kV/cm, as indicated by the dotted blue arrow in Fig. 4. By applying even higher positive electric fields the hysteresis loop starts to shift back along the μ_0H axis toward negative fields. With the application of $E=12$ kV/cm the EB becomes $\mu_0H_{\mathrm{EB}}=-6.85$ mT after magnetic field cooling to $T=40$ K. The EB shift is indicated by a dashed red arrow in Fig. 4. In addition to the electric field dependence of the EB, we have also analyzed the coercivity, H_c vs E field and found that the coercivity has a maximum value at $E=0$ kV/cm in accordance with the results reported in Ref. 44. Next we provide the theoretical framework for our findings.

We start from a phenomenological view on the electric control of EB by taking advantage of the very definition of the EB field from the left and right coercive fields of the hysteresis loops. Electric cooling-field dependence of the EB field can be traced back to the electric cooling-field dependence of the coercive fields,

$$\frac{dH_{\mathrm{EB}}}{dE}=\frac{d}{dE}\left(\frac{H_{C_{left}}+H_{C_{right}}}{2}\right)=\frac{1}{2}\left(\frac{dH_{C_{left}}}{dE}+\frac{dH_{C_{right}}}{dE}\right). \tag{1}$$

Despite the simplicity of Eq. (1) it provides already a first insight in highlighting that an E dependence of the EB field requires an asymmetric electrically induced change, $\frac{dH_{C_{left}}}{dE}\neq-\frac{dH_{C_{right}}}{dE}$, of the E dependence of the EB field.

Next we investigate in which way potential electric field dependencies of the magnetoelastic anisotropy, K_{me}, and the effective FM/AF interface exchange, J, can affect the E dependence of the EB field. With $H_{C_{left/right}}=H_{C_{left/right}}[K_{me}(E),J(E)]$ one obtains

$$\begin{aligned}\frac{dH_{\mathrm{EB}}}{dE}&=\frac{1}{2}\left(\frac{dH_{C_{left}}}{dK_{me}}\frac{dK_{me}}{dE}+\frac{dH_{C_{left}}}{dJ}\frac{dJ}{dE}\right.\\&\left.+\frac{dH_{C_{right}}}{dK_{me}}\frac{dK_{me}}{dE}+\frac{dH_{C_{right}}}{dJ}\frac{dJ}{dE}\right)\\&=\frac{1}{2}\left(\frac{dH_{C_{left}}}{dK_{me}}+\frac{dH_{C_{right}}}{dK_{me}}\right)\frac{dK_{me}}{dE}+\frac{dH_{\mathrm{EB}}}{dJ}\frac{dJ}{dE}.\end{aligned} \tag{2}$$

The average magnetoelastic anisotropy constant for a polycrystalline film $K_{me}(E)=\frac{3}{2}\sigma(E)\lambda$ depends on the average magnetostriction coefficient λ of Co and the stress $\sigma(E)$ which in turn is electric field dependent via the piezoelectric effect. A second source of electrically controlled EB is the E-field dependence of the effective interface exchange, J, between the FM and AF interface magnetization. In analogy to the E-field dependence of the magnetoelastic anisotropy constant the E-field dependence of J originates from a subtle stress dependence which can phenomenologically be expressed as $J=J[\sigma(E)]$. Such stress dependence is expected because the local atomic exchange, J_{ij}, at the interface can either be ferromagnetic for direct Co-Co exchange or antiferromagnetic if the interaction is of the superexchange type due to local oxygen termination of the AF interface.[61,68] It is reasonable to assume that the weighting and magnitude of both local interaction types can change due to stress-induced changes of the interface structure giving rise to an effective stress-dependent integral interface exchange constant.

Note that, the dependence of the EB field on the magnetoelastic anisotropy could be zero if $\left|\frac{dH_{C_{left}}}{dK_{me}}\right|=\left|\frac{dH_{C_{right}}}{dK_{me}}\right|$ meaning the K_{me} dependence of both hysteresis branches is symmetric.

Figure 5 shows that the E dependence of the left branches of the hysteresis loops is different from that of the right branches yielding a significant electric field influence on the EB field. We associate this electrically induced change primarily with a contribution from $\left|\frac{dH_{C_{left}}}{dK_{me}}\right|\neq\left|\frac{dH_{C_{right}}}{dK_{me}}\right|$ in Eq. (2). The magnetization reversal on the left branch of exchange-biased loops specifically in Co/CoO heterostructures is known to be determined by nucleation and domain wall motion while the right branch is determined by domain-wall rotation.[69–76] Due to the different mechanisms of the magnetization reversal and the general sensitive dependence of co-

ercivity on anisotropy it is reasonable that $H_{C_{left}}$ and $H_{C_{right}}$ depend dissimilarly on anisotropy changes and, hence, on the applied electric field.

The fact that the change in the EB field is manifested in first approximation by a strong reduction in the absolute value of the EB field is consistent with the expected reorientation of the Co magnetic easy axis induced by the magnetoelastic anisotropy. The reorientation of the easy axis of the Co film into out of plane gives rise to a noncollinear alignment of the FM and AF interface magnetization and, hence, reduces the EB field in qualitative agreement with the simple Meiklejohn Bean expression[77,78]

$$\mu_0 H_{\mathrm{EB}} = -\frac{J S_{\mathrm{FM}} S_{\mathrm{AF}} \cos\phi}{M_{\mathrm{FM}} t_{\mathrm{FM}}}, \tag{3}$$

where ϕ is the angle between the interface magnetizations of the FM Co layer and the AF CoO pinning layer.

In addition to the rapid electrically induced reduction in the absolute EB field for $|E|<1$ kV/cm there is a more subtle structure in the region $1<|E|<5$ kV/cm. Here the EB changes its sign and crosses into positive values. Positive EB and crossover behavior from regular into positive EB has been observed especially in Co/CoO EB system before.[79] However, those reported findings refer to temperature-dependent crossovers of the sign of the EB field. Alternatively, here we induce this crossover electrically. In all reported cases[61,80–83] of positive exchange bias there is AF interface exchange involved which allows for a competition between Zeeman and exchange energy. There are two potential mechanisms which can give rise to a sign change in the effective interface interaction, J. First, as discussed above the stress-induced local displacement of interface atoms can weaken direct Co-Co exchange in favor of indirect local Co-O-Co superexchange at oxygen-terminated interface places. Second, the theory of quantum-mechanical superexchange allows for a local crossover of the sign of exchange integrals. The latter depend strongly on the bond angle determined by overlapping orbitals. Geometric changes in these angles in molecules are known to change the exchange between positive and negative values.[84–86] While certainly a direct comparison between molecules and the complex solid-solid interface is a crude oversimplification, a fairly similar mechanism may take place at the interface of Co/CoO where the electrically induced strain changes charge distributions and hence the exchange integrals. The quantification of this mechanism requires a generalization of the theory outlined in Ref. 86. Such a generalization is a challenging step from molecules with clearly defined directed bonds to solids where itinerant exchange partners are included and outside the scope of this paper. Note that, despite being far from obvious, mapping of the energy spectra of an itinerant magnet onto a classical spin model is common practice in statistical mechanics and gives rise to the concept of exchange between localized moments in the framework of our heterostructure.[87]

We interpret our data in terms of a competition between the rotation of Co magnetization and the complex phenomenon of stress-induced superexchange coupling. In combination of these two competing mechanism the $E=0$ symmetric "butterfly" structure evolves as shown in Fig. 5. The $\mu_0 H_{\mathrm{EB}}$ vs E dependence is virtually mirror symmetric with respect to $E=0$ in agreement with $\sigma(E)=\sigma(-E)$, when hysteresis of the BTO polarization is neglected. Figure 5 is a three-dimensional (3D) graph of the overall behavior of EB vs applied electric cooling field, E, and training loop number, n for $T=40$ K. Note, that the blue mesh in Fig. 5 is an eye-guiding smooth interpolation based on the Renka-Cline algorithm which is not related to a fit of a theoretical function. Interestingly all loops trained ($n>1$) and untrained ($n=1$) show a residual E dependence of the respective EB field. The qualitative behavior displayed in Fig. 5 is consistently observed at various temperatures, $T=55$, 65, and 75 K (not shown) thus evidencing that specific details of random ferroelectric domain structures do not affect our findings.

In a given training sequence the absolute value of the EB field is at maximum for the first training loop ($n=1$). Since there is more dynamic range for a change in the EB field for $n=1$ one may expect that $\left|\frac{\Delta H_{\mathrm{EB}}}{\Delta E}(n=1)\right| > \left|\frac{\Delta H_{\mathrm{EB}}}{\Delta E}(n>1)\right|$. For example, in a training cycle at $T=40$ K the value of $\frac{\Delta H_{\mathrm{EB}}(n=1)}{\Delta E}$(=0.25 mT/kV) is about the twice of $\frac{\Delta H_{\mathrm{EB}}(n=15)}{\Delta E}$(=0.12 mT/kV). Furthermore, we explicitly evidence that in our system control of the EB requires cooling in both electric and magnetic fields. When, the sample is cooled only in magnetic fields the subsequent isothermal application of electric fields between $E=-12$ kV/cm and $E=12$ kV/cm affects neither the EB field nor the coercivity. We interpret this by the field-cooling-dependent imprinting of the CoO interface magnetization and the reduced piezoelectric response of BTO at temperatures below the blocking temperature $T_{\mathrm{B}} \approx 80$ K. In regular EB systems the spin structure of the AF pinning layer is imprinted during the magnetic cooling procedure. The magnetization of the FM layer determines via exchange how the AF interface magnetization evolves during cooling. In our BTO/Co/CoO system the magnetization state of the Co film is determined by the applied magnetic field and, simultaneously, by the orientation of the easy axis. Both factors determine the orientation of the Co magnetization. The easy-axis orientation is electrically controlled via the piezoelectrically induced stress. The FM interface magnetization is, hence, determined by the electric field and imprints the AF interface magnetization on cooling. Once the CoO interface magnetization is frozen in this mechanism is blocked and the electric field has little to no effect on the AF interface magnetization which largely controls the EB. Note that the piezoelectrically induced stress changes with maximum response between the electric coercive fields of BTO which is known, e.g., from Ref. 88 to be $|E_c| \approx 0.7$ kV/cm. This reflects the fact that the piezoelectric effect of BTO is at maximum when the system goes from a ferroelectric multidomain state into an electric field induced single-domain state. Consequently, the piezoelectrically induced change in the exchange-bias field is strongest for $|E| \leq 0.7$ kV/cm. Note that we heat the sample to above the ferroelectric critical temperature prior to each electric field cooling procedure. By doing so we lose the history dependence imprinted in the ferroelectric domain state which in an isothermal experiment would clearly be present.

In addition, isothermal piezoelectric control of the Co coercivities is not observable in our sample because the piezoelectric response in general strongly decreases with decreasing temperature and is particularly small for our BTO substrate at $T<T_B$ in the rhombohedral phase. We harness the large piezoelectric effect in the tetragonal phase at high temperatures $T \gg T_B$ thus creating significant strain on cooling. This is the reason why we have electrically controlled EB with electric freezing field. However, this strain is frozen in at target temperatures $T<T_B$ and can no longer be electrically controlled. This is the reason for the virtual absence of isothermal electric control of EB. Note that in accordance with Eq. (2) isothermal electric control of EB is expected either for larger piezoelectric effects at low temperatures or EB systems with increased blocking temperature. The virtual absence of isothermal piezoelectric control has been experimentally confirmed by us. We decided not to present these data of little relevance here.

V. CONCLUSIONS

We studied the thermal and electric field dependence of the exchange bias in ferroelectric/ferromagnetic/antiferromagnetic $BaTiO_3/Co/CoO$ heterostructure. This study is partly motivated by our earlier studies on $BaTiO_3/Fe$ where the magnetic properties of a Fe thin film can be strongly altered in proximity with a single-crystal ferroelectric.[44] It is also motivated by the technological importance of electrically controlled magnetism and exchange bias for spintronic applications. In close analogy to $BaTiO_3/Fe$, we find stress controlled magnetic anisotropy changes of the ferromagnetic Co thin film. Structural phase transitions leave their fingerprints in the Co magnetization via magnetoelastic coupling. We find electrically controlled exchange bias in $BaTiO_3/Co/CoO$ originating from dissimilar coercivity changes of the descending and ascending hysteresis loop branches. More specifically, we observe reduced exchange bias through electrically induced stress and interpret it as noncollinear relative orientation between the ferromagnetic and antiferromagnetic interface magnetizations. Further increase in electric cooling fields selects and possibly activates antiferromagnetic exchange at the Co/CoO interface through stress-induced atomic displacements. The change in the effective exchange interaction at the interface results in sign changes of the exchange-bias field. Finally, the competition between these stress-dependent mechanisms produces a symmetric butterfly structure of the electric cooling field-dependent exchange bias.

ACKNOWLEDGMENTS

This work is supported by NSF through MRSEC under Grant No. DMR-0213808 and Career No. DMR-0547887, and the Nebraska Research Initiative.

*cbinek2@unl.edu

[1] G. A. Prinz, Science **282**, 1660 (1998).
[2] A. Kingon, Nature (London) **401**, 658 (1999).
[3] L. Krusin-Elbaum, T. Shibauchi, B. Argyle, L. Gignac, and D. Weller, Nature (London) **410**, 444 (2001).
[4] S. S. P Parkin, K. P. Roche, M. G. Samant, P. M. Rice, R. B. Beyers, R. E. Scheuerlein, E. J. O'Sullivan, S. L. Brown, J. Bucchigano, D. W. Abraham, Y. Lu, M. Rooks, P. L. Trouilloud, R. A. Wanner, and W. J. Gallagher, J. Appl. Phys. **85**, 5828 (1999).
[5] J. Nogués and I. K. Schuller, J. Magn. Magn. Mater. **192**, 203 (1999).
[6] A. Berkowitz and K. Takano, J. Magn. Magn. Mater. **200**, 552 (1999).
[7] T. J. Moran, J. M. Gallego, and I. K. Schuller, J. Appl. Phys. **78**, 1887 (1995).
[8] J. Nogués, D. Lederman, T. J. Moran, I. K. Schuller, and K. V. Rao, Appl. Phys. Lett. **68**, 3186 (1996).
[9] J. Ventura, J. P. Araujo, J. B. Sousa, A. Veloso, and P. P. Freitas, Phys. Rev. B **77**, 184404 (2008).
[10] S. H. Chung, A. Hoffmann, and M. Grimsditch, Phys. Rev. B **71**, 214430 (2005).
[11] A. Hoffmann, J. Sort, K. S. Buchanan, and J. Nogués, IEEE Trans. Magn. **44**, 1968 (2008).
[12] Ch. Binek and B. Doudin, J. Phys.: Condens. Matter **17**, L39 (2005).
[13] M. Kiwi, J. Magn. Magn. Mater. **234**, 584 (2001).
[14] J. I. Hong, T. Leo, D. J. Smith, and A. E. Berkowitz, Phys. Rev. Lett. **96**, 117204 (2006).
[15] Ch. Binek, X. Chen, A. Hochstrat, and W. Kleemann, J. Magn. Magn. Mater. **240**, 257 (2002).
[16] S. Polisetty, S. Sahoo, and Ch. Binek, Phys. Rev. B **76**, 184423 (2007).
[17] M. Ali, C. H. Marrows, M. Al-Jawad, B. J. Hickey, A. Misra, U. Nowak, and K. D. Usadel, Phys. Rev. B **68**, 214420 (2003).
[18] Ch. Binek, A. Hochstrat, and W. Kleemann, J. Magn. Magn. Mater. **234**, 353 (2001).
[19] J. Kanak, T. Stobiecki1, and S. van Dijken, IEEE Trans. Magn. **44**, 238 (2008).
[20] A. Hochstrat, Ch. Binek, and W. Kleemann, Phys. Rev. B **66**, 092409 (2002).
[21] T. Hauet, J. A. Borchers, Ph. Mangin, Y. Henry, and S. Mangin, Phys. Rev. Lett. **96**, 067207 (2006).
[22] X. P. Qiu, D. Z. Yang, S. M. Zhou, R. Chantrell, K. O'Grady, U. Nowak, J. Du, X. J. Bai, and L. Sun, Phys. Rev. Lett. **101**, 147207 (2008).
[23] Ch. Binek, Phys. Rev. B **70**, 014421 (2004).
[24] A. Hoffmann, Phys. Rev. Lett. **93**, 097203 (2004).
[25] S. G. E. te Velthuis, A. Berger, G. P. Felcher, B. K. Hill, and E. Dan Dahlberg, J. Appl. Phys. **87**, 5046 (2000).
[26] Ch. Binek, S. Polisetty, X. He, and A. Berger, Phys. Rev. Lett. **96**, 067201 (2006).
[27] E. E. Fullerton, J. S. Jiang, M. Grimsditch, C. H. Sowers, and S. D. Bader, Phys. Rev. B **58**, 12193 (1998).
[28] A. Berger, D. T. Margulies, and H. Do, Appl. Phys. Lett. **85**, 1571 (2004).
[29] A. Berger, Ch. Binek, D. T. Margulies, A. Moser, and E. E. Fullerton, Physica B **372**, 168 (2006).

[30] A. Berger, O. Hovorka, G. Friedman, and E. E. Fullerton, Phys. Rev. B **78**, 224407 (2008).
[31] S. Polisetty, S. Sahoo, A. Berger, and Ch. Binek, Phys. Rev. B **78**, 184426 (2008).
[32] U. Nowak, K. D. Usadel, J. Keller, P. Miltényi, B. Beschoten, and G. Güntherodt, Phys. Rev. B **66**, 014430 (2002).
[33] R. L. Stamps, J. Phys. D **33**, R247 (2000).
[34] A. Hochstrat, Ch. Binek, X. Chen, and W. Kleemann, J. Magn. Magn. Mater. **272-276**, 325 (2004).
[35] P. Borisov, A. Hochstrat, X. Chen, W. Kleemann, and Ch. Binek, Phys. Rev. Lett. **94**, 117203 (2005).
[36] X. He, Y. Wang, N. Wu, A. N. Caruso, E. Vescovo, K. D. Belashchenko, P. A. Dowben, and Ch. Binek, Nature Mater. **9**, 579 (2010).
[37] M. Fiebig, T. Lottermoser, D. Fröhlich, A. V. Goitsev, and R. V. Pisarev, Nature (London) **419**, 818 (2002).
[38] V. Laukhin, V. Skumryev, X. Martí, D. Hrabovsky, F. Sánchez, M. V. García-Cuenca, C. Ferrater, M. Varela, U. Lüders, J. F. Bobo, and J. Fontcuberta, Phys. Rev. Lett. **97**, 227201 (2006).
[39] H. Béa, M. Bibes, F. Ott, B. Dupé, X.-H. Zhu, S. Petit, S. Fusil, C. Deranlot, K. Bouzehouane, and A. Barthélémy, Phys. Rev. Lett. **100**, 017204 (2008).
[40] W. Eerenstein, N. D. Mathur, and J. F. Scott, Nature (London) **442**, 759 (2006).
[41] R. Ramesh and N. A. Spaldin, Nature Mater. **6**, 21 (2007).
[42] M. Bibes and A. Barthelemy, IEEE Trans. Electron Devices **54**, 1003 (2007).
[43] M. Fiebig, J. Phys. D **38**, R123 (2005).
[44] S. Sahoo, S. Polisetty, C.-G. Duan, S. S. Jaswal, E. Y. Tsymbal, and Ch. Binek, Phys. Rev. B **76**, 092108 (2007).
[45] J. Wang, H. Wang, H. Jiang, X. Wang, Y. Lin, and C. W. Nan, J. Nanomater. **2010**, 142750 (2010).
[46] N. Moutis, D. Suarez-Sandoval, and D. Niarchos, J. Magn. Magn. Mater. **320**, 1050 (2008).
[47] G. Srinivasan, E. T. Rasmussen, J. Gallegos, R. Srinivasan, Yu. I. Bokhan, and V. M. Laletin, Phys. Rev. B **64**, 214408 (2001).
[48] S. Geprägs, A. Brandlmaier, M. Opel, R. Gross, and S. T. B. Goennenwein, Appl. Phys. Lett. **96**, 142509 (2010).
[49] S. Srinath, N. A. Frey, H. Srikanth, G. X. Miao, and A. Gupta, Adv. Sci. Technol. (Faenza, Italy) **45**, 2528 (2006).
[50] P. Blomqvist, K. M. Krishnan, S. Srinath, and S. G. E. te Velthuis, J. Appl. Phys. **96**, 6523 (2004).
[51] T. Brintlinger, S.-H. Lim, K. H. Baloch, P. Alexander, Y. Qi, J. Barry, J. Melngailis, L. Salamanca-Riba, I. Takeuchi, and J. Cumings, Nano Lett. **10**, 1219 (2010).
[52] M. Weiler, A. Brandlmaier, S. Geprägs, M. Althammer, M. Opel, C. Bihler, H. Huebl, M. S. Brandt, R. Gross, and S. T. B. Goennenwein, New J. Phys. **11**, 013021 (2009).
[53] M. K. Lee, T. K. Nath, C. B. Eom, M. C. Smoak, and F. Tsui, Appl. Phys. Lett. **77**, 3547 (2000).
[54] F. Zavaliche, H. Zheng, L. Mohaddes-Ardabili, S. Y. Yang, Q. Zhan, P. Shafer, E. Reilly, R. Chopdekar, Y. Jia, P. Wright, D. G. Schlom, Y. Suzuki, and R. Ramesh, Nano Lett. **5**, 1793 (2005).
[55] H. F. Kay and P. Vousden, Philos. Mag. **40**, 1019 (1949).
[56] R. G. Rhodes, Acta Crystallogr. **4**, 105 (1951).
[57] M. Gierlings, M. J. Prandolini, H. Fritzsche, M. Gruyters, and D. Riegel, Phys. Rev. B **65**, 092407 (2002).
[58] D. Tripathy and A. O. Adeyeye, Phys. Rev. B **79**, 064413 (2009).
[59] S. Brems, D. Buntinx, K. Temst, C. Van Haesendonck, F. Radu, and H. Zabel, Phys. Rev. Lett. **95**, 157202 (2005).
[60] E. Popova, H. Loosvelt, M. Gierlings, L. H. A. Leunissen, R. Jonckheere, C. Van Haesendonck, and K. Temst, Eur. Phys. J. B **44**, 491 (2005).
[61] F. Radu, M. Etzkorn, R. Siebrecht, T. Schmitte, K. Westerholt, and H. Zabel, Phys. Rev. B **67**, 134409 (2003).
[62] S. Y. Suck, V. Neu, U. Wolff, S. Bahr, O. Bourgeois, and D. Givord, Appl. Phys. Lett. **95**, 162503 (2009).
[63] S. Polisetty, J. Scheffler, S. Sahoo, Y. Wang, T. Mukherjee, X. He, and Ch. Binek, Rev. Sci. Instrum. **79**, 055107 (2008).
[64] R. P. Borges, R. C. da Silva, M. M. Cruz, and M. Godinho, J. Phys.: Conf. Ser. **200**, 072014 (2010).
[65] Y. Zhang, J. Liu, X. H. Xiao, T. C. Peng, C. Z. Jiang, Y. H. Lin, and C. W. Nan, J. Phys. D: Appl. Phys. **43**, 082002 (2010).
[66] G. E. Sterbinsky, B. W. Wessels, J.-W. Kim, E. Karapetrova, P. J. Ryan, and D. J. Keavney, Appl. Phys. Lett. **96**, 092510 (2010).
[67] H. F. Tian, T. L. Qu, L. B. Luo, J. J. Yang, S. M. Guo, H. Y. Zhang, Y. G. Zhao, and J. Q. Li, Appl. Phys. Lett. **92**, 063507 (2008).
[68] F. T. Parker, K. Takano, and A. E. Berkowitz, Phys. Rev. B **61**, R866 (2000).
[69] M. R. Fitzsimmons, P. Yashar, C. Leighton, I. K. Schuller, J. Nogués, C. F. Majkrzak, and J. A. Dura, Phys. Rev. Lett. **84**, 3986 (2000).
[70] C. Leighton, M. R. Fitzsimmons, P. Yashar, A. Hoffmann, J. Nogués, J. Dura, C. F. Majkrzak, and I. K. Schuller, Phys. Rev. Lett. **86**, 4394 (2001).
[71] C. Leighton, M. Song, and I. K. Schuller, J. Appl. Phys. **88**, 344 (2000).
[72] I. N. Krivorotov, C. Leighton, J. Nogués, I. K. Schuller, and E. D. Dahlberg, Phys. Rev. B **65**, 100402(R) (2002).
[73] C. Leighton and I. K. Schuller, Phys. Rev. B **63**, 174419 (2001).
[74] J. S. Jiang, A. Inomata, C.-Y. You, J. E. Pearson, and S. D. Bader, J. Appl. Phys. **89**, 6817 (2001).
[75] I. N. Krivorotov, C. Leighton, J. Nogués, I. K. Schuller, and E. D. Dahlberg, Phys. Rev. B **68**, 054430 (2003).
[76] A. Inomata, J. S. Jiang, C.-Y. You, J. E. Pearson, and S. D. Bader, J. Vac. Sci. Technol. A **18**, 1269 (2000).
[77] W. H. Meiklejohn and C. P. Bean, Phys. Rev. **102**, 1413 (1956).
[78] W. H. Meiklejohn and C. P. Bean, Phys. Rev. **105**, 904 (1957).
[79] T. Gredig, I. N. Krivorotov, P. Eames, and E. D. Dahlberg, Appl. Phys. Lett. **81**, 1270 (2002).
[80] J. Nogués, D. Lederman, T. J. Moran, and I. K. Schuller, Phys. Rev. Lett. **76**, 4624 (1996).
[81] F. Canet, S. Mangin, C. Bellouard, and M. Piecuch, Europhys. Lett. **52**, 594 (2000).
[82] H. Ohldag, H. Shi, E. Arenholz, J. Stöhr, and D. Lederman, Phys. Rev. Lett. **96**, 027203 (2006).
[83] C. Leighton, J. Nogués, B. J. Jönsson-Åkerman, and I. K. Schuller, Phys. Rev. Lett. **84**, 3466 (2000).
[84] S. Lebernegg, G. Amthauer, and M. Grodzicki, J. Phys.: Conf. Ser. **200**, 032039 (2010).
[85] S. Lebernegg, G. Amthauer, and M. Grodzicki, J. Phys. B **41**, 035102 (2008).
[86] S. Lebernegg, G. Amthauer, and M. Grodzicki, J. Mol. Struct. **924**, 473 (2009).
[87] M. Pajda, J. Kudrnovský, I. Turek, V. Drchal, and P. Bruno, Phys. Rev. Lett. **85**, 5424 (2000).
[88] H. H. Wieder, J. Appl. Phys. **26**, 1479 (1955).